

Effects of a constructional intervention on airborne and deposited particulate matter in the Portuguese National Tile Museum, Lisbon

Willemien Anaf · Benjamin Horemans ·
Teresa I. Madeira · M. Luisa Carvalho ·
Karolien De Wael · René Van Grieken

Received: 14 May 2012 / Accepted: 5 July 2012 / Published online: 25 July 2012
© Springer-Verlag 2012

Abstract In the 1970s, a large ambulatory of the National Tile Museum, Lisbon, was closed with glass panes on both ground and first floor. Although this design was meant to protect the museum collection from ambient air pollutants, small openings between the glass panes remain, creating a semi-enclosed corridor. The effects of the glass panes on the indoor air quality were evaluated in a comparative study by monitoring the airborne particle concentration and the extent of particle deposition at the enclosed corridor as well as inside the museum building. Comparison of the indoor/outdoor ratio of airborne particle concentration demonstrated a high natural ventilation rate in the enclosed corridor as well as inside the museum building. PM_{10} deposition velocities on vertical surfaces were estimated in the order of $3 \times 10^{-4} \text{ m s}^{-1}$ for both indoor locations. Also, the deposition rates of dark-coloured and black particles in specific were very similar at both indoor locations, causing visual degradation. The effectiveness of the glass panes in protecting the museum collection is discussed.

Keywords Preventive conservation · Airborne particulate matter · Deposition · Blackening · Museum · CC-EPMA · Ion chromatography · XRF

Responsible editor: Gerhard Lammel

W. Anaf (✉) · B. Horemans · K. De Wael · R. Van Grieken
Department of Chemistry, University of Antwerp,
Universiteitsplein 1,
2610 Antwerp, Belgium
e-mail: willemien.anaf@ua.ac.be

T. I. Madeira · M. L. Carvalho
Centro de Física Atómica, University of Lisbon,
Av. Prof. Gama Pinto 2,
1649-003 Lisbon, Portugal

Introduction

The deleterious effects of indoor airborne particulate matter (PM) for the conservation of cultural heritage are well-recognised (Tétreault 2003). Although the exact mechanisms are not yet fully understood, four different, often interrelated, types of damage can be distinguished. First of all, PM accumulation on surfaces can alter the aesthetic appearance of the object, thereby influencing the perception of the observer (Lloyd et al. 2007b; Tétreault 2003). Larger dust particles such as fibres visually contribute most to soiling (Yoon and Brimblecombe 2001), but also small particles such as soot can cause noticeable blackening (Van Grieken et al. 2000). Secondly, apart from visual degradation, mechanical damage such as enhanced abrasion could occur as well. Especially particles of high hardness, such as silicates, are able to make micro-scratches during a cleaning treatment (Ioanid et al. 2005; Wei et al. 2007), but also cleaning itself entails a risk for mechanical damage. Increased dust deposition requires more frequent cleaning, again leading to a higher risk of material deterioration through, e.g. abrasion. Since dust becomes more strongly bound to surfaces over time, some aggressive cleaning treatments might be required (Brimblecombe et al. 2009). As a third aspect, particles could transport harmful substances to indoor surfaces (Yoon and Brimblecombe 2001). Once deposited, chemical reactions between the particles and the underlying surface can fasten the degradation of many materials. For example, the moisture absorption of particles can enhance deterioration, and even inert particles could increase the presence of water on surfaces (Brimblecombe et al. 2009). Moreover, particles can act as catalysts in many degradation processes, such as the Fe-catalysed oxidation of S(IV) to S(VI) compounds (Elfving et al. 1994; Saxena and Seigneur 1987) and the absorption of reactive gases on soot,

which brings them in close proximity to the surface interface (Van Grieken et al. 2000). The fourth type of damage is bio-deterioration, induced by spores in dust, which can lead to fungal growth under favourable conditions (Ioanid et al. 2005; Prajapati 2003). On the other hand, deposited dust can form a humid micro-environment on the surface, creating a nutritional resource for fungi which aids in their survival (Caneva et al. 2008).

The present study reports on airborne and deposited PM in the Portuguese National Tile Museum (Museu Nacional do Azulejo) in Lisbon. It is one of the most important Portuguese museums, mainly due to its unique collection of tiles. The building in which the museum is lodged is the former monastery 'Madre de Deus'. Through the centuries, the building went through many restorations, especially after the 1755 earthquake. In the mid-twentieth century, the whole space was converted into a museum. In the 1970s, a considerable modification of the building was performed: the two present ambulatories were protected from the ambient atmosphere. The smallest ambulatory was fully covered with a glass roof; the biggest was closed by placing glass panes in between the pillars on both ground and first floor. The panes were intended to protect the museum collection from ambient air pollution. However, in between the panes, small openings remain, creating a semi-enclosed corridor. After the modification, clear damage was observed to the tile ensemble exposed below the glass panes. An important threat to these tiles is the direct rainwater runoff that occurs through the small openings in between the glass panes and the walls. Before the introduction of the glass panes, the rain had a certain inclination, preventing direct contact with the tiles. The tiles exposed on the opposite wall of the glass panes do not show remarkable damage. In the present study, the effectiveness of the glass panes in retaining ambient air pollution—their initial aim—was evaluated. A comparative study was performed by monitoring the air quality and the extent of particle deposition at this enclosed exposition hall as well as inside the museum building. We applied active sampling to study the concentration and composition of the coarse and fine airborne particles. Passive sampling was conducted to evaluate the deposition and blackening rate of the particles.

Materials and methods

Description of the sampling locations

The National Tile Museum is located just outside the historical centre of Lisbon, Portugal, about 500 m from the estuary of the Tagus River with the Atlantic Ocean. A railway connection and industrial park are situated in between the museum and the estuary.

The museum is housed in a historic building without central heating, ventilation and air conditioning system (HVAC). Heating and ventilation occur through several individual air conditioning systems.

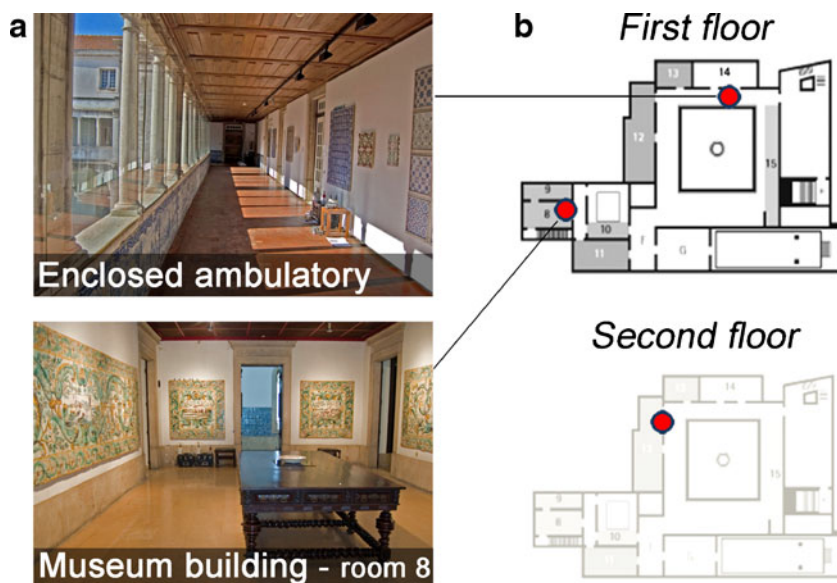
Two sampling locations were chosen on the first floor of the museum (Fig. 1). The first location was in the exposition room no. 8 of the museum building. The second location was in the big ambulatory which is enclosed with glass panes, designated below as 'enclosed exposition hall'. This was clearly connected with ambient air through narrow openings in between the glass panes. The outdoor site was located on the second floor, where the sampling equipment was placed on the outside window sills of an office.

Sampling and analysis of particulate pollutants

Winter (10 until 14 January 2011) and summer (19 until 24 September 2011) campaigns were conducted to study the composition of airborne PM₁₀ (aerodynamic diameter (AD) <10 μm) and PM_{2.5} (AD <2.5 μm). Samples were collected with MS&TTM impactors (Air Diagnostics and Engineering Inc., Harrison, ME, USA) on Teflon membrane filters (TK15-G3M, Pall, Ann Arbor, MI, USA). The PM concentration was determined by gravimetric analysis on a micro-balance (MX5, Mettler Toledo, Columbus, OH, USA). After conditioning for about 24 h (20±1 °C and 50±5 % relative humidity (RH)), the filters were weighed with an accuracy of 1 μg. Subsequently, the filters were analysed with energy dispersive X-ray fluorescence spectrometry (Epsilon-5, PANalytical, Almelo, The Netherlands) and ion chromatography (IC, DX-120, Dionex, Sunnyvale, CA, USA). Detailed description of the sampling method, analytical equipment and procedures can be found elsewhere (Horemans et al. 2008; Spolnik et al. 2005).

Passive sampling was performed to study the coverage rate of dark-coloured and black particles. To this end, samplers were made by sticking rectangular white adhesive labels on cardboard frames, thereby creating a 'sticky sampler' with a sticky surface area of 150 mm². Inside the museum building as well as at the enclosed exposition hall, 12 sticky samplers were assembled vertically on the wall at equal distances of 20 cm, covering the complete range between 10 and 230 cm above ground level (AGL). At 170 cm AGL, a Teflon filter was mounted to the wall for analysing the water-soluble fraction of deposited particles. At the same height, a filter and sticky sampler was positioned horizontally. The sampling started on 19 September 2011 for a total collection period of 3 months (94 days). Afterwards, the sticky samplers were analysed with an optical reflection microscope (Olympus BX41, Center Valley, PA, USA) using a magnification of ×600. For each sampler, 15 images were randomly collected, covering a total surface area of 18 mm². The images were converted to a binary

Fig. 1 **a** View of the enclosed ambulatory and exposition room 8 inside the museum building. **b** Floor plan of the Museo Nacional do Azulejos with indications of the sampling locations



format and subjected to automated image analysis with the ‘SigmaScan Pro’ software (Systat Software, San Jose, CA, USA). All particles were counted and the particle areas were calculated. From each particle area, a diameter of a circle of equal projection area was defined. Only dark-coloured and black particles were taken into account. Fibres were not incorporated, since they are not expected to deposit on vertically oriented non-adhesive surfaces such as glazed tiles (Yoon and Brimblecombe 2000a). The filters were analysed with gravimetry and IC in order to determine the mass and water-soluble fraction of the deposited particles, respectively.

The microclimate was monitored at both indoor locations with Hobo data loggers (Onset, Bourne, MA, USA), which measured air temperature and relative humidity every 15 min during active sampling. Outdoor meteorological data as well as PM₁₀ and PM_{2.5} concentrations were obtained from three air quality monitoring stations (Olivais, Chelas and Beato) in the measurement network of the Portuguese Environmental Agency (Agencia Portuguesa do Ambiente), each located in the vicinity of the museum.

Chemical reconstruction of PM mass

The chemical composition of airborne PM was reconstructed from the measured elements and ions. The total soil dust concentration was estimated from the elemental concentrations (in micrograms per cubic meter) by using the standard soil equation (Eq. 1) of the IMPROVE programme (Improve 2012; Malm et al. 1994). This equation accounts for the main oxides of the soil-derived elements.

$$\text{soil dust} = 2.2\text{Al} + 2.49\text{Si} + 1.63\text{Ca} + 2.42\text{Fe} + 1.94\text{Ti} \quad (1)$$

As for airborne inorganic salts, one can identify three major groups: sea salts (ss), mineral salts (min; mostly

carbonates) and ammonium salts (am). Differentiation between the contribution of each salt type cannot be made directly, since some ions are common to more than one salt. From Table 1, it can be seen that Na⁺ and NH₄⁺ ions only occur in one of the major inorganic salts of PM. Therefore, they are used as a starting point for the chemical reconstruction of each salt, by using simple assumptions on the conservation of mass and charge. It is to be mentioned here that the methodology described below always uses units expressed as charge equivalents per cubic meter, unless it is stated differently. At first, the total charge of all measured ions is balanced by adding either carbonate or hydrogen ions (Bardouki et al. 2003; Horemans et al. 2011). Secondly, the measured (*m*) amount of an ion X^{y±} is written as in Eq. 2, where the coefficient ⁱδ is 1 or 0, depending on the presence of X^{y±} in the salt type *i* (Table 1).

$$mX^{y\pm} = \sum^{ss} \delta^{ss} X^{y\pm} + \sum^{min} \delta^{min} X^{y\pm} + \sum^{am} \delta^{am} X^{y\pm} \quad (2)$$

Since the Na⁺ ion is only brought in the atmosphere by sea spray, the sea salt contribution of an ion could be estimated as ^{ss}X^{y±} = ω_X · ^mNa⁺, in which the coefficient ω_X represents the concentration (equivalents per litre) of X^{y±} relative to that of sodium in typical seawater (Cotruvo 2005). It is to be noted that the amount of nitrate and ammonium in seawater could be neglected (ω_X=0). Moreover, for reasons of mass conservation, sea spray was assumed to be the only source of an ion (^mX^{y±} = ^{ss}X^{y±}) whenever ^mX^{y±} < ω_X · ^mNa⁺.

This allows to define the airborne sea salt fraction as:

$$\text{sea salts} = \sum^{ss} \delta^{ss} X^{y\pm} + {}^{lost}Cl^{-} \quad (3)$$

The latter term in Eq. 3 arises from chloride replacement reactions between ‘genuine’ sea salts and atmospheric nitric and sulphuric acid (Laskin et al. 2003), forming ‘aged’ sea salt (ag), i.e. sodium nitrate and sulphate (^{lost}Cl⁻ = ^{ag}NO₃⁻ +

Table 1 Presence of ions in the three major inorganic salt types of airborne particulate matter

	Na ⁺	NH ₄ ⁺	K ⁺	Mg ²⁺	Ca ²⁺	NO ₃ ⁻	SO ₄ ²⁻	Cl ⁻
Genuine+aged sea salts (ss)	x		x	x	x	x	x	x
Genuine+aged mineral salts (min)			x	x	x	x	x	x
Ammonium salts (am)		x				x	x	x

x: present

^{ag}SO₄²⁻). Its magnitude is chosen so that it compensates for the anion deficit in the sea salt contributions of all ions, i.e. $\text{lostCl}^- = \sum^{\text{ss}} \delta^{\text{ss}} X^{y+} - \sum^{\text{ss}} \delta^{\text{ss}} X^{y-}$. The amount of aged nitrate and sulphate can be differentiated from ammonium salts when it is assumed that (1) atmospheric ammonia first neutralises all available sulphuric acid before reacting with nitric acid (Seinfeld 1986a) and (2) nitric acid will react preferentially with sea salts before forming ammonium nitrate:

$$\text{If } m\text{SO}_4^{2-} \leq m\text{NH}_4^+ + \text{H}^+ \\ \text{then } \begin{cases} \text{amNO}_3^- = m\text{NH}_4^+ + \text{H}^+ - m\text{SO}_4^{2-} \\ \text{amSO}_4^{2-} = m\text{SO}_4^{2-} \end{cases} \text{ else } \begin{cases} \text{amNO}_3^- = 0 \\ \text{amSO}_4^{2-} = m\text{NH}_4^+ + \text{H}^+ \end{cases} \quad (4)$$

$$\text{If } m\text{NO}_3^- \leq \text{lostCl}^- \text{ then } \begin{cases} \text{agNO}_3^- = m\text{NO}_3^- \\ \text{agSO}_4^{2-} = \text{lostCl}^- - m\text{NO}_3^- \end{cases} \text{ else } \begin{cases} \text{agNO}_3^- = \text{lostCl}^- \\ \text{agSO}_4^{2-} = 0 \end{cases} \quad (5)$$

From which, the quantitative expressions for the amount of ammonium and mineral salts result:

$$\text{ammonium salts} = \sum^{\text{am}} \delta^{\text{am}} X^{y\pm} + \text{H}^+ \quad (6)$$

$$\text{mineral salts} = \sum^{\text{min}} \delta^{\text{min}} X^{y\pm} + \text{CO}_3^{2-} \quad (7)$$

The mineral components are obtained by:

$$\text{min } X^{y\pm} = m X^{y\pm} - \text{am } X^{y\pm} - \text{ss } X^{y\pm} (-\text{ag } X^{y\pm}). \quad (8)$$

Results and discussion

Airborne particulate matter

Figure 2 summarises the mass concentration and chemical composition of coarse (PM_{10-2.5}) and fine (PM_{2.5}) airborne PM as observed inside the museum building, at the enclosed exposition hall as well as outdoors. The concentration and composition of both PM fractions at the two indoor locations are similar to that observed outdoors. The small differences could result from individual events such as movements of people, cleaning, heating, cooling, etc.

The coarse fraction is rich in sea salts and soil dust, which contributed on average to about 57±4 % of the total PM mass. The abundance of soil dust in Lisbon is often affected by episodic Saharan dust outbreaks (Almeida et al. 2007).

Therefore, the NOAA HYSPLIT Saharan dust dispersion model (HYSPLIT 2012) was used to evaluate Saharan dust events. During the active sampling, no Saharan dust intrusions were predicted and PM₁₀ concentrations were maximally 30 μg m⁻³. However, during passive sampling, the model predicted a Saharan dust intrusion which lasted for about 3 days (12–14 November), during which, the total PM₁₀ concentration, obtained from a nearby weather station, reached up to 54 μg m⁻³. In total, about 16 days during passive sampling were found with average PM₁₀ values above 50 μg m⁻³. Hence, apart from Saharan dust intrusions, other sources of mineral dust, such as construction works, local emissions, etc., were thought to be considerable as well. The fine PM fraction was mainly composed of ammonium salts. The unexplained mass in both fractions could be (partly) attributed to organic and elemental carbon and aerosol-associated water, which were not systematically analysed.

The average indoor-to-outdoor (*I/O*) concentration ratios at the museum locations are around unity for both coarse and fine PM (Table 2), indicating a high natural ventilation rate. Specific aerosol types show similar *I/O* ratios, with only minor exceptions (Table 2). Both sea salts and minerals in airborne PM originate typically from outdoors. Indoors, the amount of sea salt in the coarse fraction was less than outside, while indoor coarse minerals were comparable to the amount found outdoors. Thus, apart from the natural penetration of particles in the museum building, minerals are expected to have an additional way to infiltrate into the museum, e.g. via visitors (Van Grieken et al. 2000; Yoon and Brimblecombe 2000a). Results from Yoon and Brimblecombe (2000a) demonstrated that the amount of soil dust which was brought inside through the shoes of museum visitors was the highest when relative humidity was high. This was certainly the case during the present winter campaign, for which an average RH of 92 % was obtained in the ambient air.

Fine soil and sea salts had somewhat higher *I/O* ratios compared to the coarse fraction (Table 1). Coarse particles are indeed partially obstructed by the building, while fine PM can more easily infiltrate and eventually accumulate. Although the ammonium salts appear in the fine fraction and are therefore expected to easily infiltrate into the museum, the *I/O* ratio is slightly below 1. This can be due to the dissociation of volatile ammonium nitrate at elevated indoor temperatures (compared to outdoor temperatures, it was on average 4.9±0.9 and

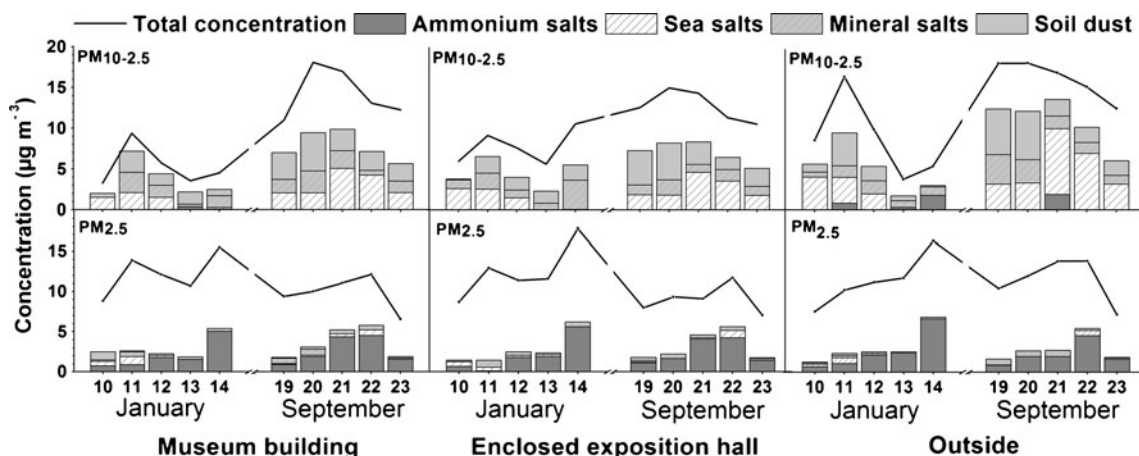


Fig. 2 Mass and composition of airborne PM_{10-2.5} and PM_{2.5}

5.6±1.3 °C warmer in the museum building and the enclosed exposition hall, respectively). Moreover, the formed nitric acid is sorbed by indoor surfaces (e.g. walls) at a much faster rate than ammonia, which accumulates (Lunden et al. 2003). This sink for nitric acid makes the dissociation of NH₄NO₃ to proceed more easily. The loss could be illustrated by the sulphate-to-nitrate equivalent ratio in ammonium salts. Outdoors, the average ratio was found to be 3.1, while indoor averages of 7.6 and 9.5 were found inside the museum building and the enclosed exposition hall, respectively, clearly indicating the loss of ammonium nitrate.

Deposited particulate matter

The total mass of deposited PM was the highest on horizontal surfaces (Fig. 3), mainly due to gravitational settling of large particles (Kildeso et al. 1999). The strong contribution of coarse particles in the deposition samples is evident from the composition, which is rich in sea salts and mineral salts (most abundant in coarse PM_{10-2.5}) and poor in ammonium salts (most abundant in fine PM_{2.5}). Since small sea salt particles (high surface/volume ratio) age more rapidly compared to larger ones (Laskin et al. 2003), vertical surfaces will be enriched with aged sea salts as compared to horizontal surfaces. Indeed, sea salts which deposited on vertical

surfaces were found to be highly aged (29–46 %), while aged sea salts on horizontal surfaces represented less than 6 % of the total deposited sea salt fraction.

Deposition of particles smaller than 0.1 µm is governed by Brownian and turbulent motion, while particles larger than 1 µm deposit mainly through gravitational settling and inertial impaction. Hence, the deposition rate of particles is found to be minimal for intermediate-sized particles, i.e. between 0.1 and 1.0 µm (Lai 2002; Seinfeld 1986b). Earlier studies have demonstrated that ammonium-rich particles are most abundant in this intermediate size range (e.g. Ferm et al. 2006; Alves et al. 2007, and references therein), and thus, although they were considerably present in airborne PM_{2.5}, they were hardly found in deposited PM samples (Fig. 3). This is consistent with the results of Nazaroff et al. (1990), from which it was concluded that the fraction of fine particles (0.05–2 µm) depositing on museum walls was not more than 1 %. Moreover, after deposition, these particles could dissociate due to temperature gradients or react with deposition surfaces and with other deposited particles such as carbonates (Ferm et al. 2006; Mori et al. 1998). Sea salts and minerals are mainly present in coarse PM (>2 µm), so their deposition velocity is considerably higher. Although surface reactions with gaseous pollutants can still occur after deposition (Ferm et al. 2006), the composition of airborne and deposited sea salt and mineral particles was rather comparable.

Table 2 Average (± confidence interval of 95 %) indoor-to-outdoor concentration ratios for airborne PM and specific aerosol types

	Enclosed exposition hall			Museum building		
	PM _{2.5}	PM _{10-2.5}	PM ₁₀	PM _{2.5}	PM _{10-2.5}	PM ₁₀
Total	1.0±0.1	0.9±0.2	0.9±0.1	1.0±0.1	0.8±0.1	0.91±0.05
Soil dust	1.6±0.5	0.9±0.2	0.9±0.2	1.5±0.4	1.2±0.3	1.2±0.2
Sea salts	1.1±0.2	0.61±0.06	0.68±0.09	1.2±0.2	0.68±0.08	0.73±0.08
Ammonium salts	0.8±0.2	n.a.	0.7±0.2	0.92±0.09	n.a.	0.7±0.2

n.a. not applicable

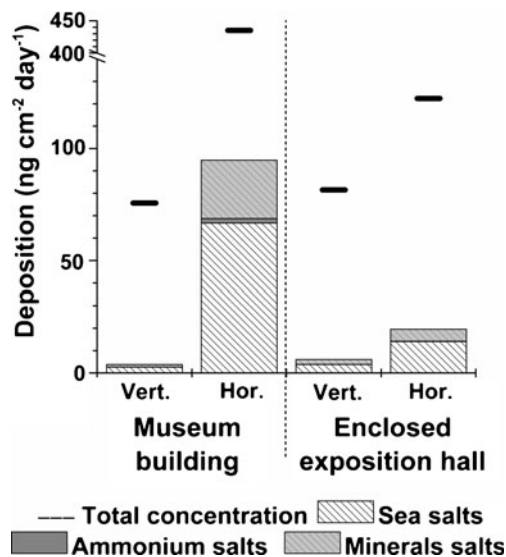


Fig. 3 Deposited PM on horizontal and vertical surfaces

Deposition rate and velocity

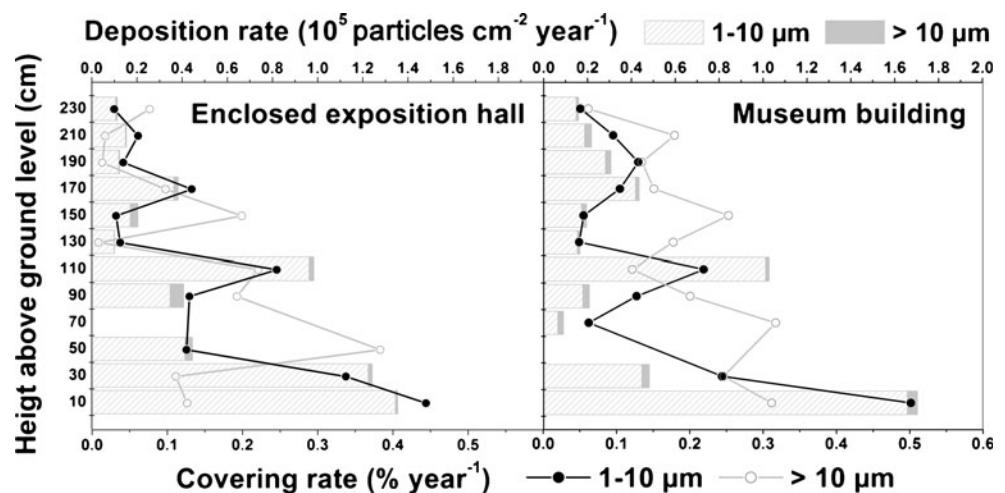
The vertical deposition profiles of dark-coloured or black particles were very similar at both indoor locations (Fig. 4). The profiles agree well with the results of Yoon and Brimblecombe (2000b, 2001) and those from Knight (2004). The sticky surface that was used as a collection substrate has the advantage that particles cannot easily detach from the sample. However, it was estimated by Yoon and Brimblecombe (2000a) that the fluxes determined with sticky samplers are approximately three times higher than by using non-adhesive substrates. Therefore, the deposition rate on the tile surfaces in the museum is expected to be considerably lower than estimated in Fig. 4.

The particle covering area was used to segregate particles according to size: diameters between 1 and 10 μm and larger than 10 μm . Although particles $>10 \mu\text{m}$ were rare, they contributed remarkably to the total surface covering. However,

since such large particles barely deposit on non-adhesive vertical surfaces such as the majority of tiles in the museum (mounted to the walls), particles within the size fraction of 1–10 μm were believed to be most relevant in the present study. For this particle fraction, deposition was found to be high close to the ground level ($0.5\text{--}1.7 \times 10^{-5}$ particles cm^{-2} year $^{-1}$ up to 30 cm AGL). This can be related to the suspension of soil dust which easily occurs on the stone floor, present at both locations. Visitors as well as a turbulent environment can cause particle suspension. Suspension generally affects particles larger than 1 μm , since smaller particles are attracted more to the floor by Van Der Waals forces (Yoon and Brimblecombe 2000a). Around 110 cm, another increase in the deposition rate (about 1.0×10^{-5} cm^{-2} year $^{-1}$) is observed, which is also known to be caused by visitors (Yoon and Brimblecombe 2001). Deposition on the horizontally mounted sticky sampler at the enclosed exposition hall (covering fraction of 7.6 %) was remarkably higher compared to the corresponding sampler inside the museum building (covering fraction of 4.3 %), which was mainly due to some large particles which could be visually observed.

One of the most important parameters related to the deposition of particles is the relative covering area, i.e. the fraction of the surface which is covered by dark (light absorbing) particles. Once a critical covering area is exceeded, blackening of the cultural artefact becomes visible to the naked eye. Carey (1959) suggested that soiling of black particles on a white surface becomes visible once the coverage area exceeds a value of 0.2 %. Under the conditions observed at the tile museum, this means that soiling on the white tiles would be visible at floor and chest levels only after 1 year of soiling (Fig. 3). Bellan et al. (2000) report a threshold value of 12 % coverage area and 3.6 % when a clean and soiled surface are positioned edge to edge, since non-uniform soiling will more rapidly lead to a noticeable visual degradation (Nazaroff et al. 1990). When extrapolating the present results, a coverage area of 3.6 % would be reached at the chest level after 14–15 years (sticky surface).

Fig. 4 Vertical profiles for the deposition and covering rate of dark-coloured and black particles



Although surface covering can be useful in understanding the extent of soiling, there are still some weaknesses in the use of it. First of all, it is dependent on the type of particles. Both Carey (1959) and Bellan et al. (2000) used black particles on idealised surfaces to predict the critical value of a perceptible surface covering. However, due to differences in light-absorbing properties and morphology, different types of blackening particles (mostly soot and soil dust) will have a different value for the critical surface covering (Nazaroff and Cass 1991; Nazaroff et al. 1990). Secondly, surface covering could not be estimated by making a simple linear extrapolation. At first, the area covered progresses linearly; however, since particles start to overlap, the covering rate slows down and eventually reach a constant value. Lloyd et al. (2007a) introduced an empirical scale that correlates the perception of dustiness with the percentage coverage area. According to this study, a horizontal surface is perceived as ‘fairly dusty’ from a 6–7 % coverage area. Following this dustiness perceptions, the enclosed exposition hall can already be considered as fairly dusty after only 3 month of exposure of the sticky sampler (horizontal surface coverage=7.6 %). Though, this study focuses on horizontal surfaces and does not discriminate in particle colour, shape and size. Therefore, the covering will partly originate from coarse particles such as fibres. These particles can easily be distinguished by the human eye, since they clearly contrast with the deposition surface. However, a similar coverage area, formed by fine particles spread over the surface, will be perceived in a different way. This will be the case for the vertically oriented tiles. Therefore, more research is needed to obtain a more realistic idea on the concept of vertical surface covering and the time needed to reach an observable degree of soiling.

The average deposition velocity of airborne PM₁₀ and specific aerosol types was calculated from the amount of deposited PM and the average indoor concentration of airborne PM₁₀ (Table 3). Since the latter was not measured

over the complete period of passive sampling, it was estimated from the average outdoor concentration obtained from nearby air quality monitoring stations and the average PM₁₀ indoor-to-outdoor ratios (Table 2). Horizontally mounted samples were not taken into account, since the very large particles on these filters are not representative for airborne PM₁₀. The deposition velocity for PM₁₀ on vertical surfaces was in the order of $0.3 \times 10^{-3} \text{ m s}^{-1}$ at both locations, which agrees quite well with results of Piskunov (2009) and Lai (2002). For ammonium salts, a negligibly low deposition velocity was obtained for both locations, i.e. $0.002 \times 10^{-3} \text{ m s}^{-1}$.

Conclusion

At the enclosed exposition hall as well as in the museum building, the indoor/outdoor ratios were near unity, which indicates a high natural ventilation rate. Coarse particles are partly obstructed from infiltrating into the museum, but fine particles (e.g. black carbon) have virtually no difficulty to infiltrate into the indoor environment, where they can soil the museum artefacts. Since (glazed) ceramic is considered to be a relative stable material, soiling is not expected to result in chemical alterations of the museum collection; however, visual degradation or ‘blackening’ should be considered. Experimentally determined deposition rates for vertical oriented surfaces were nearly equal at both locations in the museum with an average PM₁₀ deposition rate of $0.3 \times 10^{-3} \text{ m s}^{-1}$. Dark-and black-coloured particles have remarkably higher deposition rates at floor and chest level, with deposition of up to 1.6×10^5 particles $\text{cm}^{-2} \text{ year}^{-1}$. In general, slightly higher deposition rates were observed inside the building. On the other hand, deposition on horizontal surfaces is remarkably higher at the

Table 3 Vertical deposition velocities (v_d) for airborne PM₁₀ and specific aerosol types

	Enclosed exposition hall		Inside			
	Concentration ^a	v_d^b	Concentration ^a	v_d^b		
	($\mu\text{g m}^{-3}$)	($\times 10^{-3} \text{ m s}^{-1}$)	($\mu\text{g m}^{-3}$)	($\times 10^{-3} \text{ m s}^{-1}$)		
	Mean	CI	Mean	CI		
PM ₁₀	30±3	0.296	0.267–0.334	30±2	0.316	0.300–0.335
Mineral salts	3±1	0.055	0.033–0.079	2.9±0.7	0.058	0.047–0.075
Sea salts	3.3±0.4	0.092	0.081–0.106	3.5±0.4	0.124	0.112–0.139
Ammonium salts	3.4±0.9	0.002	0.002–0.003	4±1	0.002	0.001–0.002

CI confidence interval (95 %)

^a Average concentration for the passive sampling period, estimated from the outdoor PM₁₀ concentrations, considering the indoor/outdoor ratios during the active sampling campaign.

^b Range of deposition velocities, based on the confidence interval of the airborne particle concentration.

enclosed exposition hall, which was most probably due to a higher concentration of coarse particles ($AD > 10 \mu\text{m}$).

The glass panes in the ambulatory exposition halls are not effectively protecting the museum collection from ambient air pollution (and from airborne particles in specific). Since the glass panes are not well-sealed to the stone construction, rainwater infiltrates into the ambulatory, causing direct damage to a series of tiles and enhancing mold and fungi growth. Moreover, the panes enhance temperature and humidity variations caused by direct sunlight. Improving the indoor air quality for the conservation of the collection can be obtained in two ways: (1) by removing all glass panes. This will prevent the direct damage due to rainwater runoff. Furthermore, extreme heating will be avoided. The indoor concentration of pollutants will increase only slightly, not entailing serious conservation threats. (2) By sealing the openings between the panes, thereby reducing the air exchange rate with ambient air. This will decrease airborne particle concentrations and thus soiling. However, greenhouse effects will be significant, introducing the need of a good ventilation and air purification system, which are expensive, not always efficient, and often demand some constructional intervention which is not always possible in a historical building. Both solutions can change the microclimate and air turbulence within the museum, so any intervention should be accompanied by detailed studies.

Acknowledgments We are thankful to all the staff of the National Tile Museum for the friendly welcome and assistance during the sampling campaigns.

References

- Almeida SM, Farinha MM, Ventura MG, Pio CA, Freitas MC, Reis MA, Trancoso MA (2007) Measuring air particulate matter in large urban areas for health effect assessment. *Water, Air, Soil Pollut* 179:43–55
- Alves C, Pio C, Campos E, Barbedo P (2007) Size distribution of atmospheric particulate ionic species at a coastal site in Portugal. *Quim Nova* 30:1938–1944
- Bardouki H, Liakakou H, Economou C, Sciare J, Smolik J, Zdimal V, Eleftheriadis K, Lazaridis M, Dye C, Mihalopoulos N (2003) Chemical composition of size-resolved atmospheric aerosols in the Eastern Mediterranean during summer and winter. *Atmos Environ* 37:195–208
- Bellan LM, Salmon LG, Cass GR (2000) A study on the human ability to detect soot deposition onto works of art. *Environ Sci Technol* 34:1946–1952
- Brimblecombe P, Thickett D, Yoon YH (2009) The cementation of coarse dust to indoor surfaces. *J Cult Heritage* 10:410–414
- Caneva G, Nugari MP, Salvadori OE (2008) Plant biology for cultural heritage, biodeterioration and conservation. Getty Conservation Institute, Los Angeles
- Carey WF (1959) Atmospheric deposition in Britain—a study of dinginess. *Int J Air Pollut* 2:1–26
- Cotruvo JA (2005) Water desalination processes and associated health and environmental issues. *Water Cond Purif* 47:13–17
- Elfving P, Panas I, Lindqvist O (1994) Model study of the 1st steps in the deterioration of calcareous stone. 3. Manganese and iron-mediated sulfation of natural stone. *Appl Surf Sci* 78:373–384
- Ferm M, Watt J, O’hanlon S, De Santis F, Varotsos C (2006) Deposition measurement of particulate matter in connection with corrosion studies. *Anal Bioanal Chem* 384:1320–1330
- Horemans B, Worobiec A, Buczynska A, Van Meel K, Van Grieken R (2008) Airborne particulate matter and BTEX in office environments. *J Environ Monit* 10:867–876
- Horemans B, Cardell C, Bencs L, Kontozova-Deutsch V, De Wael K, Van Grieken R (2011) Evaluation of airborne aerosols at the Alhambra Monument in Granada, Spain. *Microchem J* 99:429–438
- HYSPLIT (2012) <http://www.ciecem.uhu.es/hysplit/index.php>. Accessed April 2012
- Improve (2012) <http://vista.cira.colostate.edu/improve>. Accessed April 2012
- Ioanid GE, Parpauta D, Vlad AM (2005) The electrostatic behaviour of materials used in restoration-conservation process. *J Optoelectron Adv Mater* 7:1643–1649
- Kildeso J, Vallarino J, Spengler JD, Brightman HS, Schneider T (1999) Dust build-up on surfaces in the indoor environment. *Atmos Environ* 33:699–707
- Knight B (2004) Dust in historic houses: conservation and management. *Engl Heritage Conserv Bull* 45:18–20
- Lai ACK (2002) Particle deposition indoors: a review. *Indoor Air* 12:211–214
- Laskin A, Gaspar DJ, Wang WH, Hunt SW, Cowin JP, Colson SD, Finlayson-Pitts BJ (2003) Reactions at interfaces as a source of sulfate formation in sea-salt particles. *Science* 301:340–344
- Lloyd H, Bendix C, Brimblecombe P, Thickett D (2007a) Dust in historic libraries, museum microclimates. *The National Museum of Denmark, Copenhagen*, pp 135–144
- Lloyd H, Brimblecombe P, Lithgow K (2007b) Economics of dust. *Stud Conserv* 52:135–146
- Lunden MM, Revzan KL, Fischer ML, Thatcher TL, Littlejohn D, Hering SV, Brown NJ (2003) The transformation of outdoor ammonium nitrate aerosols in the indoor environment. *Atmos Environ* 37:5633–5644
- Malm WC, Sisler JF, Huffman D, Eldred RA, Cahill TA (1994) Spatial and seasonal trends in particle concentration and optical extinction in the United States. *J Geophys Res-Atmos* 99:1347–1370
- Mori I, Nishikawa M, Iwasaka Y (1998) Chemical reaction during the coagulation of ammonium sulphate and mineral particles in the atmosphere. *Sci Total Environ* 224:87–91
- Nazaroff WW, Salmon LG, Cass GR (1990) Concentration and fate of airborne particles in museums. *Environ Sci Technol* 24:66–77
- Nazaroff WW, Cass GR (1991) Protecting museum collections from soiling due to the deposition of airborne particles. *Atmos Environ Gen Top* 25:841–852
- Piskunov VN (2009) Parameterization of aerosol dry deposition velocities onto smooth and rough surfaces. *J Aerosol Sci* 40:664–679
- Prajapati CL (2003) Accumulation of solid particles on documents, a threat for preservation of documentary heritage—the example of the National Archives of India. *Restaurator-International Journal for the Preservation of Library and Archival Material* 24:46–54
- Saxena P, Seigneur C (1987) On the oxidation of SO_2 to sulfate in atmospheric aerosols. *Atmos Environ* 21:807–812
- Seinfeld JH (1986a) Thermodynamics of aerosols and nucleation theory, atmospheric chemistry and physics of air pollution. Wiley, New York, pp 343–390
- Seinfeld JH (1986b) Atmospheric removal processes and residence times, atmospheric chemistry and physics of air pollution. Wiley, New York
- Spolnik Z, Belikov K, Van Meel K, Adriaenssens E, De Roeck F, Van Grieken R (2005) Optimization of measurement conditions of an

- energy dispersive X-ray fluorescence spectrometer with high-energy polarized beam excitation for analysis of aerosol filters. *Appl Spectrosc* 59:1465–1469
- Tétreault J (2003) Key airborne pollutants. In: Tétreault J (ed) *Airborne pollutants in museums, galleries, and archives. Risk Assessment, Control Strategies, and Preservation Management* Canadian Conservation Institute, Ottawa, pp 7–19
- Van Grieken R, Gysels K, Hoornaert S, Joos P, Osan J, Szaloki I, Worobiec A (2000) Characterisation of individual aerosol particles for atmospheric and cultural heritage studies. *Water Air Soil Pollut* 123:215–228
- Wei W, Joosten I, Keim K, Douna H, Mekking W, Reuss M, Wagemakers J (2007) Experience with dust measurements in three Dutch museums. *Zeitschrift für Kunsttechnologie und Konservierung* 21:261–269
- Yoon YH, Brimblecombe P (2000a) Contribution of dust at floor level to particle deposit within the Sainsbury Centre for Visual Arts (UK). *Stud Conserv* 45:127–137
- Yoon YH, Brimblecombe P (2000b) Dust at Felbrigg Hall. *Views* 32:31–32
- Yoon YH, Brimblecombe P (2001) The distribution of soiling by coarse particulate matter in the museum environment. *Indoor Air* 11:232–240